ELSEVIER

Computers in Biology and Medicine 38 (2008) 611–619

Computers in Biology and Medicine

www.intl.elsevierhealth.com/journals/cobm

Automatic segmentation of age-related macular degeneration in retinal fundus images

Cemal Köse[a,*], Uğur Şevik[a], Okyay Gençalioğlu[b]

[a]*Department of Computer Engineering, Faculty of Engineering, Karadeniz Technical University, 61080 Trabzon, Turkey*
[b]*Faculty of Medicine, Karadeniz Technical University, 61080 Trabzon, Turkey*

Received 20 June 2007; accepted 21 February 2008

Abstract

Every year an increasing number of people are affected by age-related macular degeneration (ARMD). Consequently, vast amount of information is accumulated in medical databases and manual classification of this information is becoming more and more difficult. Therefore, there is an increasing interest in developing automated evaluation methods to follow up the diseases. In this paper, we have presented an automatic method for segmenting the ARMD in retinal fundus images. Previously used direct segmentation techniques, generating unsatisfactory results in some cases, are more complex and costly than our inverse method. This is because of the fact that the texture of unhealthy areas of macula is quite irregular and varies from eye to eye. Therefore, a simple inverse segmentation method is proposed to exploit the homogeneity of healthy areas of the macula rather than unhealthy areas. This method first extracts healthy areas of the macula by employing a simple region growing method. Then, blood vessels are also extracted and classified as healthy regions. In order to produce the final segmented image, the inverse image of the segmented image is generated as unhealthy region of the macula. The performance of the method is examined on various qualities of retinal fundus images. The segmentation method without any user involvement provides over 90% segmentation accuracy. Segmented images with reference invariants are also compared with consecutive images of the same patient to follow up the changes in the disease.

Keywords: Medical image processing; Retina; Optic disk; Macula; Age-related macular degenerations; Segmentation; Diagnosis

1. Introduction

In this paper, an automatic segmentation method is developed to measure the area of the age-related macular degenerations (ARMDs) in the retinal fundus images [1–3]. The biggest challenge for segmentation of macular degenerations is the in-homogeneity of textures in macular region and uncertainty of borders between different lesions. In other words, the most common problems encountered during segmentation of lesions are due to the non-uniformity of the ARMD. These problems arise mostly because of differences in the development of ARMD.

ARMD is one of the most common retinal diseases. It may even result in blindness for people over the age of 65. Retinal fundus imaging allows the evaluation of ARMD. However, segmenting and measuring enlargement of ARMDs are quite difficult because of their irregular structures. As a consequence, large number of clinical experiments may be needed to overcome these difficulties. Recent researches have shown that pathological lesions such as ARMD can be measured from retinal fundus images [1,4]. Therefore, quantifying these problems will enable the evaluation of course of diseases. Consequently, there is a strong demand to automate the measurement and diagnosis processes.

Current methods for the measurement of the lesions in ARMD, based on some form of segmentation, require the involvement of a trained clinician [4–6]. Actually, the segmentation is carried out by a clinician [7–11]. If there is any degeneration in the macular area, the boundary of degeneration is manually traced as in Fig. 1(c). Here, the scans are obtained as

* Corresponding author: Tel.: +90 4623773167; fax: +90 4623257405.
E-mail addresses: ckose@ktu.edu.tr (C. Köse), usevik@ktu.edu.tr (U. Şevik), okyaygenc@meds.ktu.edu.tr (O. Gençalioğlu).

0010-4825/$ - see front matter © 2008 Elsevier Ltd. All rights reserved.
doi:10.1016/j.compbiomed.2008.02.008

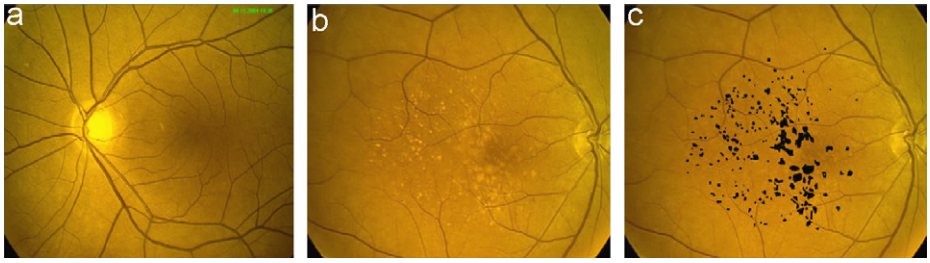

Fig. 1. Images of (a) a healthy, (b) an unhealthy and (c) a manually segmented unhealthy macula.

color images from a fundus camera. A clinician visually inspects and identifies the presence of degenerations in the images. The unhealthy area of the macula can be estimated by summing the segmented unhealthy areas. The process can take up to half an hour for both eyes of a patient. This manual method requires considerable experience to obtain accurate results and is also subject to bias in the judgment of the clinician.

Currently, a number of automated segmentation and analysis methods for retinal diseases are available [1,2,12–16]. These methods usually require quite sophisticated user input to initialize the procedure and determine the macular region before the automated segmentation process.

The rest of this paper is organized as follows. An overview of implementation details of the developed system is given in Section 2. The segmentation method for the ARMD is explained in the same section. The measurement and evaluation methods for ARMD are presented in Section 3. Implementation and results are discussed in Section 4. Conclusion and future work are given in Section 5.

2. Segmentation of ARMD

In practice, to measure the degeneration several color retinal fundus images are taken from the eyes of a patient using special digital cameras. Sometimes, these images are taken periodically to follow up the results of medical treatments applied to a patient. In our applications, these images are first converted to 8-bit grayscale images and then segmentation processes are applied to measure the eye degeneration. Measuring these retinal degenerations, other structural degenerations and the changes of the degenerations in the course of time is quite hard and laborious for an ophthalmologist. The quality of the images may not also be good enough for an ophthalmologist. Therefore, a simple inverse region growing method is employed, which enables us to segment and measure the lesions of ARMD in retinal fundus images automatically.

When degeneration is diagnosed in an eye, ophthalmologists apply a medical treatment according to the size of degeneration. They also want to measure the changes of degeneration in time after medical treatment is applied. Since the proposed method measures the size of changes, they can evaluate the results more easily by using this method. Hence, they can check whether the medical treatment is effective or not. Then, they may also arrange the dosage of drugs according to the results if necessary.

The segmentation method involves several steps that can be monitored by user. In the first step, healthy regions of the macula excluding vessels are segmented by employing proposed method. Then, blood vessels and other healthy areas in the macula are segmented to measure the unhealthy areas accurately. Finally, the inverse of the segmented areas are taken to determine unhealthy regions of the macula. Here, unhealthy regions could also have been segmented directly, like the other methods, to measure and evaluate the ARMD. But, this approach generates less accurate results, compared to our method, because the texture of unhealthy areas of the macula is quite irregular and it varies from eye to eye and from illness to illness, which makes segmentation process more complex and costly. Therefore, rather than the direct method, this proposed indirect approach is applied because it generates more accurate segmentation results.

The basic steps in automatic segmentation of ARMD are (1) choosing a sample healthy area in the image, (2) obtaining the statistical properties of the healthy textures around the macula, (3) detecting the optic disk and determination of the macula, (4) applying the region growing segmentation method to segment healthy areas in the macula, (5) eliminating the vessels in the interested region, (6) generating the inverse segmentation of the segmented image, (7) calculating percentages of healthy and unhealthy areas of the interested region, (8) comparing the segmentation results of images obtained on previous occasions, and finally (9) generating quantitative results to diagnose the disease and measure healing. A flowchart of the ARMD segmentation in retinal fundus images is given in Fig. 2.

2.1. Detecting the optic disk

In literature, several techniques are used to detect the optic disk in a retinal fundus image [14,17–20]. Optic disks in the retinal fundus images have many distinctive properties that can be used in their detection. These properties are their high intensity, circular geometric structure, the structure of blood vessels, etc. In this application, a vertical Sobel filter is employed as an edge detection filter to detect the optic disk vertically [19,21]. Then, the intensity changes and edges around the optic disk are used to determine the vertical location of optic disk [13,22–26]. Especially vessels in and around optic disk, and their intensity changes may be used to locate optic disk in a retinal fundus image. Here, the filter makes the edges on the image more evident. A histogram of the filtered image is calculated as illustrated in Fig. 3. The maximum values of histograms are used to determine the position of optic disk. The histogram of the

vertical stripe around the optic disk as illustrated in the figure is only considered to calculate horizontal position of the optic disk. If there is some degeneration around the optic disk, the result may be a misdetection. To reduce the misdetection rate, an experimentally determined threshold value is used. Therefore, the histograms are calculated by considering only pixels with intensity values in a determined interval. Thus, only the intensity distributions of optic disk and vessels are considered rather than the intensity distribution of degenerations.

2.2. Locating the macula

The macula may easily be located by detecting the optic disk, if images are taken at certain scale, angle and position. The relative locations of optic disk and macula and the distance between these invariants can be used to locate the macula. If retinal fundus images are taken from a certain position, the macula in left and right eyes can be located on right or left side of the image easily. Hence, location of the macula is determined by considering the location of optic disk, and the relative distance between optic disk and macula. Therefore, firstly, whether the location of macula is on the right or left side of the image is determined, and then experimental information such as relative positions and distances is used to locate the macula more precisely. If the optic disk is close to the left side of image, the macula is on the right. Otherwise, the macula is on the left.

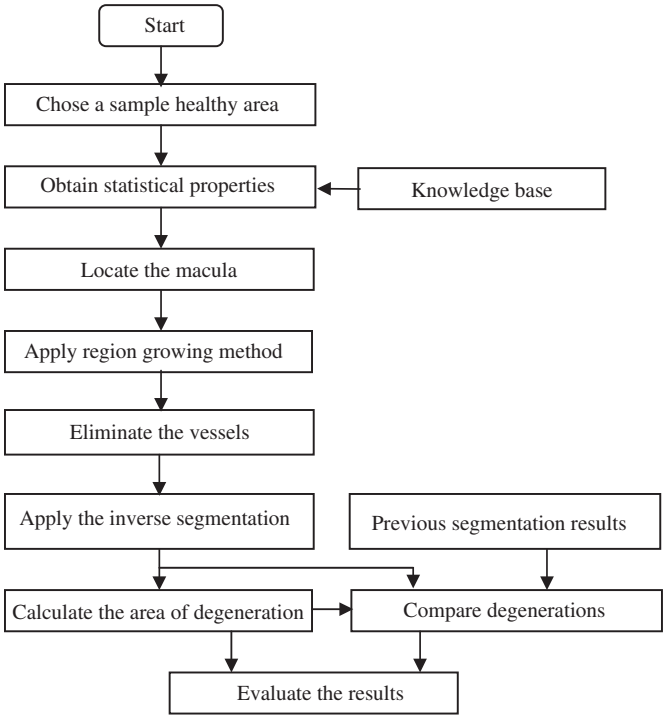

Fig. 2. The flowchart of the essential steps in the segmentation of the macular degeneration.

2.3. Region growing method

Region growing approach iteratively merges regions around the initial set of small areas according to similarity constraints. The region growing method starts by choosing an arbitrary pixel as seed and searches for similar neighboring pixels. Then, it enlarges the seed pixel by adding similar neighboring pixels. When one region stops growing, another seed pixel which does not yet belong to any region is chosen and the same process is applied again. Thus, whole process is performed until all pixels belong to a region. In this implementation, the region growing technique uses the average intensity and standard deviation to segment images. Here, each seed pixel is compared with the neighboring pixels. If they have the same distribution, and difference between the seed and neighboring pixels is in an expected interval, the pixel is segmented as healthy. After that, the region growing method, given in Eq. (1), is used to segment healthy regions in the macula. To segment the whole image, each neighboring pixel's intensity value is compared with the average intensity value of the currently segmented area. Fig. 4 shows the segmentation performance of the inverse region growing method.

$$\text{Segment}(R) = \begin{cases} \text{Healthy} & \text{if } |\text{Pix\_Cur}(j,k) - \mu_\mu| \leqslant \Delta, \\ \text{Unhealthy} & \text{otherwise\_or\_vessel}, \end{cases} \quad (1)$$

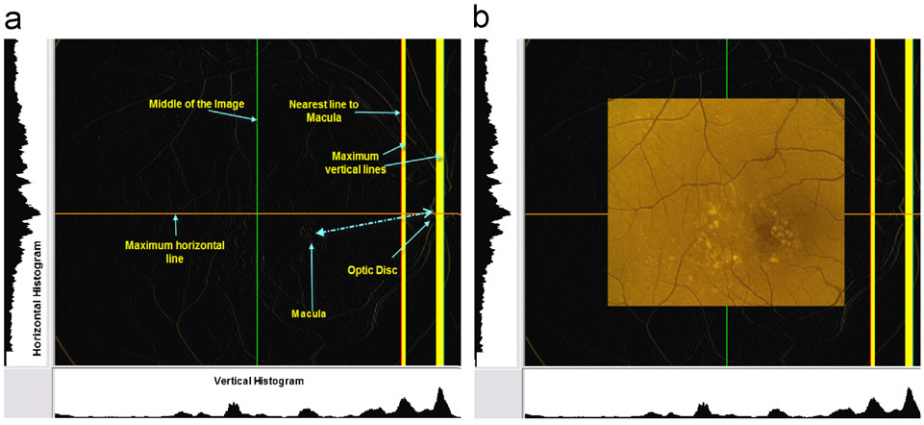

Fig. 3. (a) Detecting optic disk and (b) locating macula in a retinal fundus image.

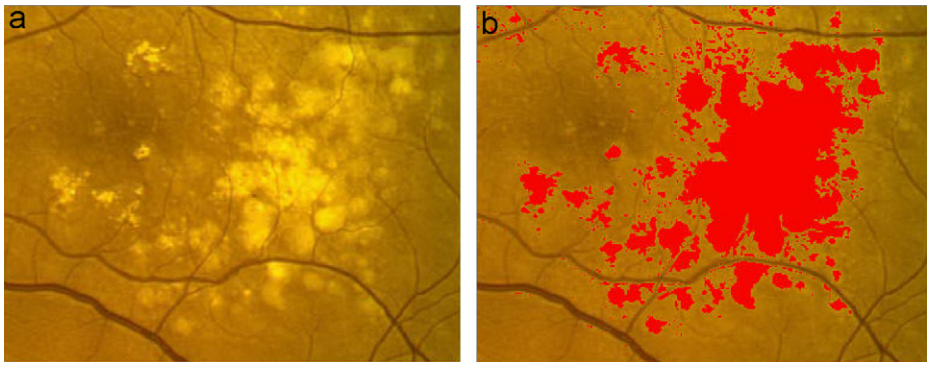

Fig. 4. (a) An original image and (b) segmented results by using the region growing method.

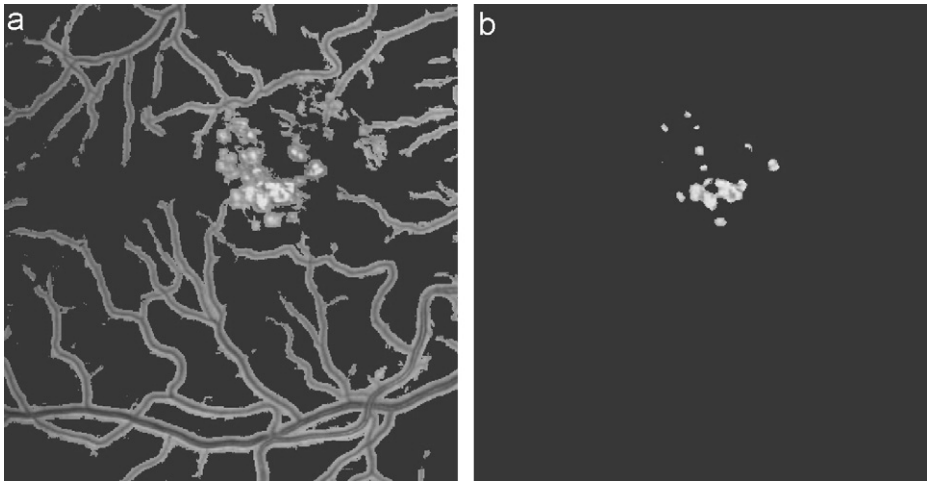

Fig. 5. (a) A segmented image with vessels and (b) vessels eliminated by using the simple vessel segmentation method.

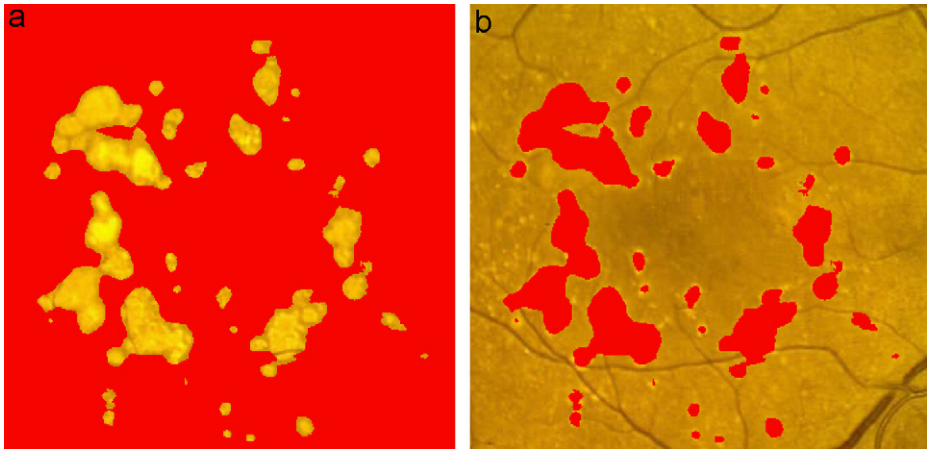

Fig. 6. (a) A segmented image and (b) the inverse of the segmented image.

where Segment(R) is the segmentation results, Pix_Cur(j, k) represents the intensity of the current pixel, μ_μ represents the average of the currently segmented pixels and Δ represents the reference threshold.

2.4. The vessel elimination

The macular region contains mostly capillary vessels which are short and narrow rather than long and large [12,16,27]. If these vessels are not eliminated correctly, they may be accounted as ARMD. Thus, these vessels have to be eliminated to increase the accuracy of the final segmentation. In practice, we found that vessels around the healthy regions mostly have relatively low intensity than the pixels around it. The total area of these regions is also smaller than the rest in the macula. Therefore, these low intensity parts of the images should also be segmented as healthy texture. Here, a simple method that calculates the average intensity and standard deviations of a

group of un-segmented pixels is employed to eliminate these regions in a macula. If the group's average intensity is within the expected interval, these pixels are segmented as blood vessel and set as healthy texture as shown in Fig. 5. Otherwise the pixels are set as unhealthy. Finally, inverse segmentation is applied to the whole segmented image to segment the unhealthy regions of the macula.

2.5. The inverse segmentation

Practically, we expect that almost the whole healthy textures are segmented and then the inverse of segmented image would include all of the unhealthy regions in the macula. Therefore, the inverse of segmented image is taken to generate the targeted segmentation result. In other words, unhealthy regions are determined based on healthy area by inverse segmentation.

Here, an important question to be asked is that "Why unhealthy regions haven't been segmented directly?" The answer to this question is that unhealthy textures of macula differ quite dramatically in terms of size and texture according to our experiments. On the other hand, healthy textures of the macula do not vary that much. Direct segmentation results also show that direct segmentation of unhealthy areas is not as much successful as the indirect segmentation, shown in Fig. 6. Therefore, we applied the indirect method to segment the unhealthy areas of macula.

3. Measurement and evaluation of ARMD

In the medical department, ophthalmologists have to deal with large amount of retinal fundus images everyday. Thus, an automatic segmentation method may enable them to more rapidly analyze these images. In this paper, a simple method is presented to segment and measure ARMDs in retinal fundus images. This proposed method automatically generates a complete segmentation of unhealthy areas in macular area in a retinal fundus image.

Several approaches are employed for segmenting and measuring ARMDs in retinal fundus images. Comparison of the accuracies of these approaches may be problematic due to the differences in scanned images, textures of the healthy and unhealthy regions of the macula, and evaluation methods. A manual segmentation of the degeneration on a retinal image is presented in Fig. 7. The proposed method performs inverse region growing based on average intensities of pixel texture, and standard deviation of intensities. An automatically segmented image is given in Fig. 8.

3.1. Comparison of the segmentation results

Manual segmentation and measurement of ARMD is quite difficult and tedious, and user may easily make mistakes in the segmentation [28–30]. Quality of segmentation also changes depending on the variation in the image and user's qualifications. Here, a simple comparison method is used to measure the ARMD. A comparison method is also required to measure

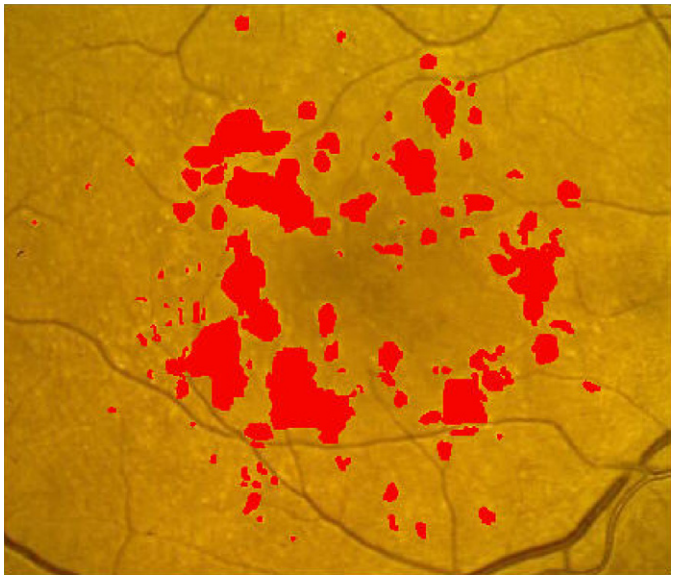

Fig. 7. A manually segmented image.

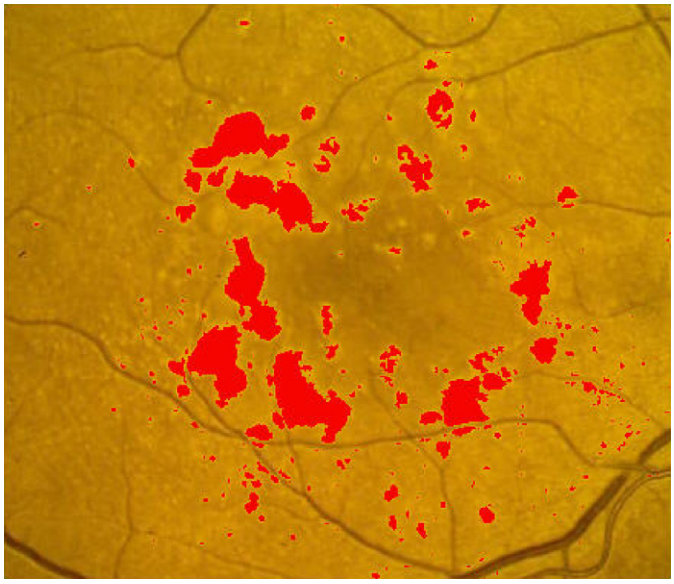

Fig. 8. An inverse segmented image by using the region growing method.

recovery of patient at certain period of the medical treatment. In this application, Eq. (2) is used to measure the size of degenerations.

$$\text{Deg\_Area} = \sum_{i=1}^{M}\sum_{j=1}^{N}\{\text{Pixel}(i,j)\}\cdot \text{seg}, \tag{2}$$

where Deg_Area is the degenerated area in the macula, Pixel(i, j) stands for the pixels in the area and is set to 1, and seg represents the segmentation results. Here, seg is 1 for segmented pixels and 0 for other pixels.

$$\text{Seg\_Error} = \sum_{i=1}^{M}\sum_{j}^{N}\text{seg\_cmp}_{(i,j)}, \tag{3}$$

where Seg_Error is the segmentation error when both segmentation results are compared with each other. Here, $seg\_cmp_{(i,j)}$ is 1 if corresponding pixels have the same segmentation results. Otherwise it is set to 0.

Here, Eq. (3) is used to compare results of the segmentations. Monitoring effectiveness of an applied medical treatment is important, and Eq. (3) is used to measure the differences between segmented images taken in previous occasions.

3.2. Measuring the ARMD

Automatic measurement of the ARMD is preferable because it avoids inter/intra-observer variability and it better suits for clinical studies and measurements. The areas of ARMD are also calculated by searching the pixels in the macula segmented as unhealthy. Hence, the system calculates the degenerated area. If the degenerated area is larger than an experimentally determined threshold value, the degeneration is diagnosed as positive. Hence, ophthalmologist may take the patient into further examination and apply proper medical treatment to heal the degeneration.

4. Results

In this paper, an automatic method is presented to segment and measure the ARMD. Experiments were performed to determine the accuracy of the method. During the study, about 60 retinal color images were obtained from the digital fundus camera situated at Department of Ophthalmology, at Faculty of Medicine, in Karadeniz Technical University. Typically, several images were taken from each patient before and after medical treatment. Two samples from those images are shown in Fig. 9. Images taken from a patient before and after treatment are shown in Figs. 9(a) and (b) and their segmentation results are presented in Figs. 9(c) and (d), respectively. For testing, all of the images with various difficulties were chosen as the training set including 15 images before medical treatment and 15 images after medical treatment. The segmentation system was run on PC with P4-3.2 GHz CPU and 512 MB RAM. For segmentation, all of the test images are processed in 3.86 min on the system. The results prove that our approach is quite promising for large-scale mining applications as well.

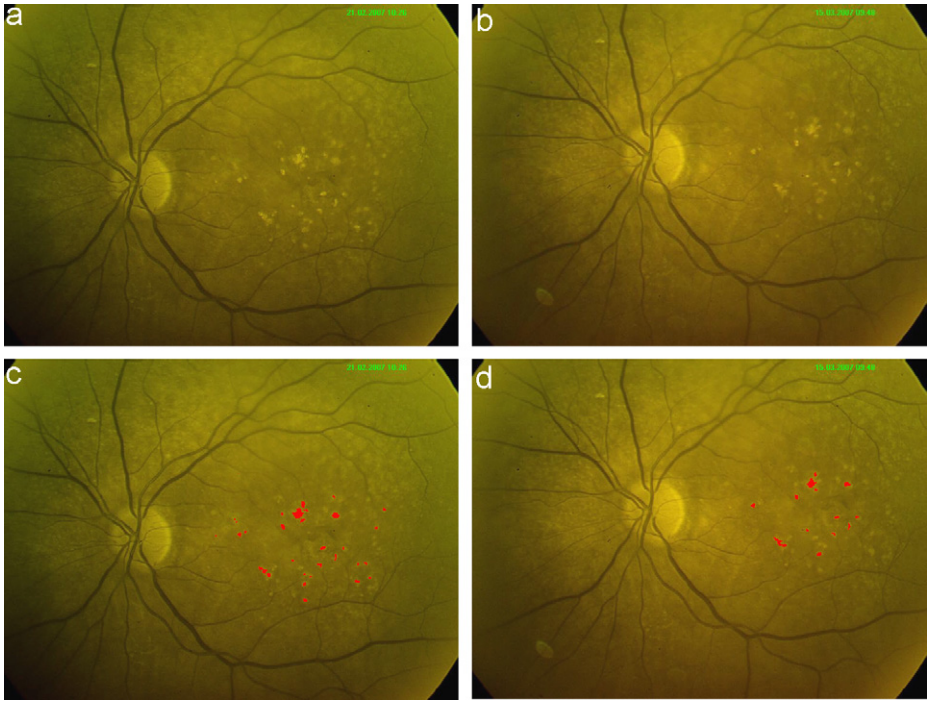

Fig. 9. (a) First and (b) second images taken from a patient to follow up the medical treatment, and (c) and (d) segmentation results of the first and second images, respectively.

Table 1
Detecting optic disk and locating the macula

	Number of images	Locating optic disk (in %)	Locating macula using the optic disk (in %)	Overall performance (in %)
Images with no degeneration	30	100	100	100
Images with degeneration	30	96.6	96.6	96.6
Overall performance	60	98.3	98.3	98.3

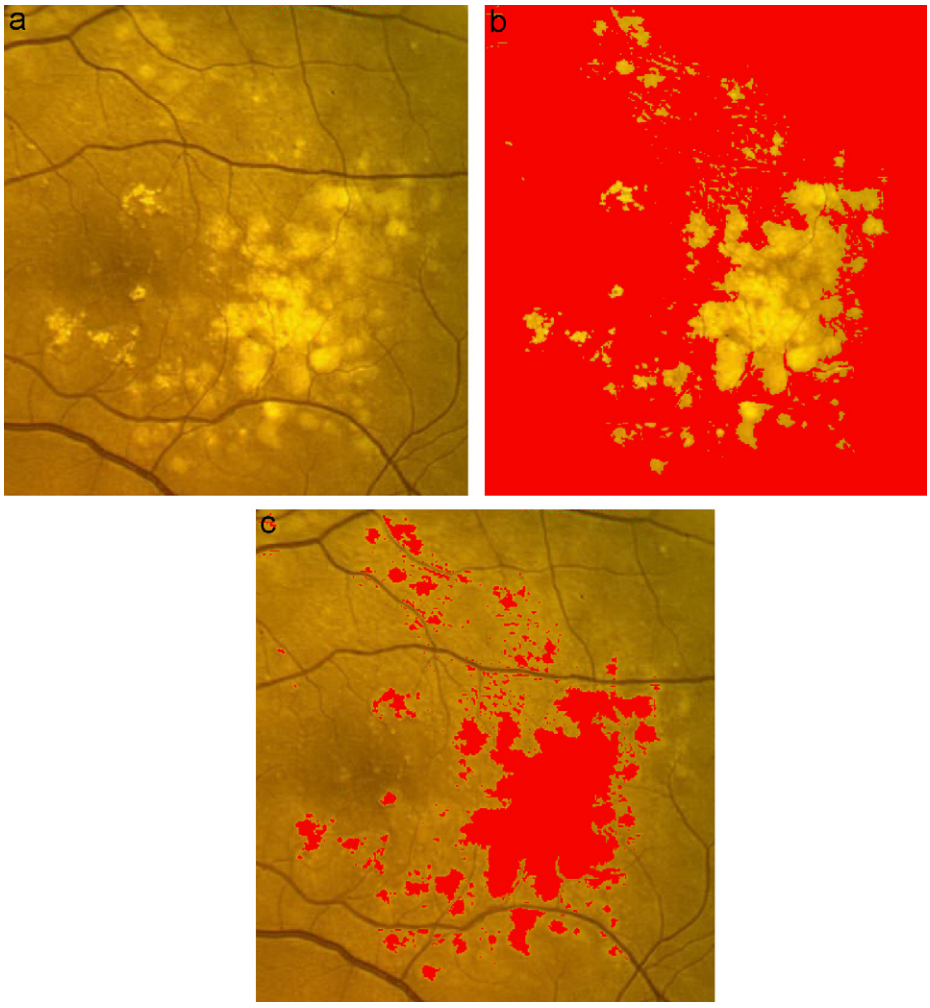

Fig. 10. (a) An original image, (b) normal and (c) inverse segmentation results of the image.

Experimental results for detecting and locating the macula are given in Table 1. These results show that all optic disks on the images with no degeneration are detected successfully and whole macular area is also located successfully. On the other hand, 96% of the optic disk in the images with degenerations is detected successfully. Thus, the general performance of the system is about 98%. Fig. 10 shows an original retinal fundus image, the segmented image by region growing method and the inverse segmentation of the segmented image.

The accuracy of both segmentation and measurement was determined by comparing the degenerated retinal areas segmented by our method with those segmented manually. Here, the accuracy of segmentation is determined by a threshold. The difference between manual segmentation and automatic segmentation shows the segmentation accuracy.

Performance of the segmentation methods is given in Table 2. In the table, first five lines show performances of the approaches applied on individual images with small-, medium- and large-scale degenerations. A comparison between manual method and our automatic method for ARMD measurement is given in the table. These results prove that the manual and automatic methods show quite similar performances in measuring the degenerations in the macula. In addition to this, our automatic segmentation method can reduce the processing time significantly. Initial testing indicated that processing an image automatically takes less than 10 s, which takes 10–40 min when manual method is used.

The results prove that the proposed method shows a high segmentation and measurement accuracy. This simple segmentation method is also an efficient approach to follow up the changes in the ARMD. In this respect, the performances of the segmentation methods are given in Table 3. In this table, first six lines show performances of the manual and region growing methods on individual images with various degenerations. These results show that the proposed method is quite useful to follow up the changes of the disease.

In most cases, the segmentation method works fine and little or no adjustments are required to correct the outline. Manual and region growing segmentation results of retinal fundus images with degeneration or no degeneration are given in Table 4. The proposed segmentation method with vessels elimination gives average accuracy which is about 92%. Here, this automatic method does not require user interaction and practical results show that it is quite suitable for clinical studies and medical treatments.

Table 2
A comparison of the manual and region growing segmentation results

	Manually segmented areas	Segmented area by using region growing	Non-overlapping segmentations	Overlapping segmentations (in %)
Sample image 1	441	385	56	87.30
Sample image 2	1199	1328	129	89.24
Sample image 3	4340	4726	386	91.11
Sample image 4	16 989	18 072	1083	93.63
Sample image 5	24 156	25 376	1220	94.95
Average for 30 images	9576	10 335	759	92.07

Table 3
Segmentation to follow up the changes of the disease

	First image	Second image	No overlapping	Changes (in %)
Manual segmentation of image 1	955	523	432	+45.24
Region growing on image 1	841	431	410	+48.75
Manual segmentation of image 2	373	456	−83	−22.25
Region growing on image 2	316	379	−63	−19.93
Manual segmentation of image 3	874	1020	−146	−16.70
Region growing of image 3	769	876	−107	−13.91
Manual segmentation of 15 images	882	799	83	+ 9.4
Region growing on 15 images	767	690	77	+10.0

Table 4
The diagnosis performance of the methods

	Number of images	Area of the degenerations (in %)	Accuracy of the segmentation (in %)
Manual segmentation of healthy retinal fundus images	20	0	100
Region growing on healthy retinal fundus images	20	3–4	96–97
Manual segmentation of unhealthy retinal fundus images	20	1–70	70–90
Region growing on unhealthy retinal fundus images	20	1–70	85–97

5. Conclusion and future work

Previously, several direct methods are employed to segment and measure ARMDs in retinal images [1,2,15,26,31]. These direct methods are limited by at least one of the following drawbacks. Firstly, user involvement may be needed to select the region of interest. Secondly, under varying image conditions, lack of adaptive capabilities of the methods may result in poor segmentation such as over and/or under segmentations in some parts of the image. Thirdly, these methods may not eliminate capillaries and vessels in the macula successfully. Lastly, ARMD segmentation process may require large computational effort.

In this study, a fast automatic segmentation approach has been developed for quantifying the ARMD. In order to do this, we addressed a simple inverse segmentation method for measuring the macular degenerations in retinal fundus images. The direct segmentation methods are more complex and expensive than the proposed method because the texture of unhealthy areas of macula is quite irregular. Therefore, in this application, the proposed inverse segmentation method is employed since it generates more accurate results than other direct segmentation methods. This proposed approach has also the ability to extract blood vessels in the macular area.

The method, evaluated on 60 retinal fundus images, achieves higher segmentation accuracy than other methods do [1,2,26,31]. It also has the ability to extract the healthy, unhealthy areas, and the blood vessels. Using the method, the complete analysis of an image can be done in several seconds without any user involvement. The method is quite satisfactory in terms of segmentation and measurement accuracy. The system achieves accuracy over 90%. These results also show that the threshold may vary from image to image. As a future work, more clinical tests and experiments need to be done to choose more precise threshold value for an interested image. There are also a few cases where our automatic method leads to incorrect segmentation. As another future work, our goal is to improve our system to overcome this problem.

Based on our experiments, we suggest that the method may also be applied in segmentation of other textures. Therefore, another future task is to apply this method in segmentation of other conditions such as diabetic retinopathy and other lesions.

Conflict of interest statement

None declared.

Acknowledgments

The digital color fundus magnetic images were provided by Faculty of Medicine at Karadeniz Technical University. We would like to thank staff and members of the faculty for providing the data sets used in this study. The authors also would like to thank Prof. Dr. Hidayet Erdöl for his contributions on medical issues in this study.

References

[1] W.E. Hart, B. Cote, P. Kube, M. Goldbaum, M. Nelson, Automatic Segmentation and Classification of Objects in Retinal Images, Computer Science and Engineering University of California, San Diego, 1994.
[2] K. Rapantzikos, M. Zervakis, Nonlinear enhancement and segmentation algorithm for the detection of age-related macular degeneration (AMD) in human eye's retina, in: Proceedings of International Conference on Image Processing, 2001, vol. 3, 2001, pp. 1055–1058.
[3] T. Walter, J.C. Klein, P. Massin, A. Erginay, A contribution of image processing to the diagnosis of diabetic retinopathy—detection of exudates in color fundus images of the human retina, IEEE Trans. Med. Imag. 21 (2002) 1236–1243.
[4] R. Chrastek, M. Wolf, K. Donath, et al., Automated segmentation of the optic nerve head for diagnosis of glaucoma, Med. Image Anal. 9 (4) (2005) 297–314.
[5] S. Huh, T.A. Ketter, K.H. Sohn, et al., Automated cerebrum segmentation from three-dimensional sagittal brain MR images, Comput. Biol. Med. 32 (5) (2002) 311–328.
[6] M.M.J. Letteboer, O.F. Olsen, E.B. Dam, P. Willems, M.A. Viergever, W.J. Niessen, Segmentation of tumors in MR brain images using an interactive multi-scale watershed algorithm, Acad. Radiol. 11 (2004) 1125–1138.
[7] J.A. Lynch, S. Zaim, J. Zhao, A. Stork, C.G. Peterfy, H.K. Genant, Cartilage segmentation of 3D MRI scans of the osteoarthritic knee combining user knowledge and active contours, in: Proceedings of SPIE, vol. 3979, 2000, pp. 925–935.
[8] S.S. Mohamed, M.M.A. Salama, Spectral clustering for TRUS images, Biomed. Eng. Online 6 (2007), Art. No.: 10.
[9] N. Moon, E. Bullitt, K. van Leemput, G. Gerig, Automatic brain and tumor segmentation, in: MICCAI, LNCS, 2002.
[10] J.G. Tamez-Pena, S. Totterman, K.J. Parker, Unsupervised statistical segmentation of multispectral volumetric MRI images, in: Medical Imaging: Image Processing, Proceedings of the SPIE, vol. 3661, 1999, pp. 300–311.
[11] M.F. Tolba, M.G. Mostafa, MR-Brain image segmentation using Gaussian multiresolution analysis and the EM algorithm, in: International Conference on Enterprise Information Systems (ICEIS), 2003, pp. 165–170.
[12] M. Al-Rawi, M. Qutaishat, M. Arrar, An improved matched filter for blood vessel detection of digital retinal images, Comput. Biol. Med. 37 (2) (2007) 262–267.
[13] J. Folkesson, E.B. Dam, P.C. Pettersen, M. Nielsen, O.F. Olsen, C. Christiansen, Locating articular cartilage in MR images, in: Medical Imaging 2005: Image Processing, Proceedings of the SPIE, 2005.
[14] C. Sinthanayothin, J.F. Boyce, H.L. Cook, T.H. Williamson, Automated location of the optic disk, fovea, and retinal blood vessels from digital colour fundus images, Br. J. Ophthalmol. 83 (8) (1999) 902–909.
[15] C.V. Stewart, Computer vision algorithms for retinal image analysis: current results and future directions, Lecture Notes in Computer Science, vol. 3765, Springer, Berlin, 2005, pp. 31–50.
[16] K.A. Vermeer, F.M. Vos, H.G. Lemij, et al., A model based method for retinal blood vessel detection, Comput. Biol. Med. 34 (3) (2004) 209–219.
[17] G. Kom, A. Tiedeu, M. Kom, Automated detection of masses in mammograms by local adaptive thresholding, Comput. Biol. Med. 37 (1) (2007) 37–48.
[18] H. Li, O. Chutatape, Automatic location of optic disk in retinal images, in: Proceedings of the IEEE-ICIP, vol. 2, 2001, pp. 837–840.
[19] A. Osareh, M. Mirmehdi, B. Thomas, R. Markham, Comparison of color spaces for optic disc localization in retinal images, in: Proceedings of the 16th IEEE International Conference on Pattern Recognition, vol. 1, 2002, pp. 743–746.
[20] J.A. Xu, O. Chutatape, Auto-adjusted 3-D optic disk viewing from low-resolution stereo fundus image, Comput. Biol. Med. 36 (9) (2006) 921–940.
[21] I. Pitas, A.N. Venetsanopoulos, Nonlinear Digital Filters: Principles and Applications, Kluwer Academic Publishers, Dordrecht, 1990.
[22] M. Lalonde, M. Beaulieu, L. Gagnon, Fast and robust optic disk detection using pyramidal decomposition and Hausdorff-based template matching, IEEE Trans. Med. Imag. 20 (2001) 1193–1200.
[23] F. Mendels, C. Heneghan, P.D. Harper, R.B. Reilly, J.-Ph. Thiran, Extraction of the optic disk boundary in digital fundus images, [Engineering in Medicine and Biology, 1999, 21st Annual Conf. and the 1999 Annual Fall Meeting of the Biomedical Engineering Soc.] BMES/EMBS conference, 1999. Proceedings of the first Joint, vol. 2, 1999, pp. 1139.
[24] J.T. Song, Z.R. Chi, Z.Y. Wang, et al., Locating human eyes using edge and intensity information, Lecture Notes in Computer Science, vol. 3645, 2005, pp. 492–501.
[25] A. Villeger, L. Ouchchane, J.C. Lemaire, et al., Data fusion and fuzzy spatial relationships for locating deep brain stimulation targets in magnetic resonance images, Lecture Notes in Computer Science, vol. 4179, 2006, pp. 909–919.
[26] M. Wilson, P. Soliz, S.C. Nemeth, Computer-aided methods for quantitative assessment of longitudinal changes in retinal images presenting with maculopathy, Medical Imaging 2002, vol. 4681, 2002, pp. 150–170.
[27] C. Köse, Fully automatic segmentation of coronary vessel structures in poor quality X-ray angiograms images, Lecture Notes in Computer Science, vol. 4109, Springer, Berlin, 2006, pp. 72–82.
[28] T.W. Nattkemper, T. Twellmann, H. Ritter, et al., Human vs. machine: evaluation of fluorescence micrographs, Comput. Biol. Med. 33 (1) (2003) 31–43.
[29] S.K. Pakin, J.G. Tamez-Pena, S. Totterman, K.J. Parker, Segmentation, surface extraction and thickness computation of articular cartilage, SPIE, Medical Imaging, vol. 4684, 2002, pp. 155–166.
[30] T. Stammberger, F. Eckstein, M. Michaelis, K.-H. Englmeier, M. Reiser, Interobserver reproducibility of quantitative cartilage measurements: comparison of B-spline snakes and manual segmentation, Magn. Reson. Imaging 17 (1999) 1033–1042.
[31] K. Rapantzikos, M. Zervakis, K. Balas, Detection and segmentation of drusen deposits on human retina: potential in the diagnosis of age-related macular degeneration, Med. Image Anal. 7 (1) (2003) 95–108.

Cemal Köse was born in Trabzon, Turkey, in 1964. He received the B.Sc. and M.Sc. degrees from the Karadeniz Technical University, Turkey, in 1986 and 1990, respectively. He received a Ph.D. degree from the University of Bristol, UK, in 1997. Since 1997, he has been with the Karadeniz Technical University, Turkey, where he is Assistant Professor in Department of Computer Engineering at the Karadeniz Technical University. His research interests focus on medical image processing, pattern recognition and information extraction.

Uğur Şevik was born in Mersin, Turkey, in 1981. He received the B.Sc. degree from the Karadeniz Technical University, Turkey, in 2003. Since 2004, he has been with the Karadeniz Technical University, Turkey, where he is Research Assistant in Department of Statistics and Computer Sciences. His research interests focus on medical image processing, pattern recognition and biomedical engineering.

Okyay Gençalioğlu was born in Istanbul, Turkey, in 1980. He received the B.Sc. degree from the Karadeniz Technical University, Turkey, in 2002. Since 2002, he has been with the Karadeniz Technical University, Turkey, where he is Medical Software Programmer Assistant in Medical Faculty. His research interests focus on medical image processing, pattern recognition and biomedical engineering.